

ARTICLES

Transient Absorption Studies of the Photochromic Behavior of 3H-Naphtho[2,1-*b*]pyrans Linked to Thiophene Oligomers via an Acetylenic Junction

Baptiste Moine,^{*,†,||} Julien Réhault,[†] Stéphane Aloïse,[†] Jean-Claude Micheau,[§] Corinne Moustrou,[‡] André Samat,[‡] Olivier Poizat,^{*,†} and Guy Buntinx[†]

Laboratoire de Spectrochimie Infrarouge et Raman (UMR 8516 du CNRS), Centre d'Etudes et de Recherches Lasers et Applications (FR 2416 du CNRS), Université des Sciences et Technologies de Lille, Bât C5, 59655 Villeneuve d'Ascq Cedex, France, Laboratoire des IMRCP (UMR 5623 du CNRS), Université Paul Sabatier, 118 Route de Narbonne, 31062 Toulouse Cedex, France, and Groupe de Chimie Organique et Matériaux Moléculaire (UMR 6114 du CNRS), Université de la Méditerranée, Faculté des Sciences de Luminy, Case 601, 13288 Marseille Cedex 09, France

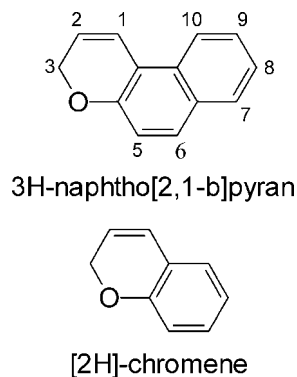
Received: December 18, 2007; Revised Manuscript Received: February 26, 2008

The photophysical and photochemical properties of four 3,3-diphenyl-3H-naphtho[2,1-*b*]pyrans substituted, via an acetylenic junction, to (thiophene)_{*n*} oligomers (*n* = 0–3 units) were investigated by transient absorption in the femtosecond to microsecond time domain and by stationary absorption and fluorescence. The decay of the initially produced excited S₁(ππ*) state is found to occur via three competing processes: fluorescence, intersystem crossing, and a ring-opening reaction leading to a colored merocyanine product, with relative yields varying drastically with *n*. Whereas ultrafast (sub-picosecond) reaction dynamics and high product quantum yield are observed for *n* = 0 and 1, the reaction is considerably slowed down on going to the *n* = 2 (105 ps) compound and does not occur for *n* = 3. A reaction scheme that accounts for this behavior is proposed and the effect of the oligothiophenic chain length on the photoinduced properties is discussed. It is suggested that increasing the chain length from 1 to 3 thiophene units stabilizes the S₁(ππ*) state by π conjugation and induces an excited-state potential barrier along the reaction pathway.

Introduction

The aim of molecular electronics is to use individual molecules as functional building blocks for nanometer-scale electrical circuits.^{1–3} Single-molecule devices appear to be ideal candidates for future nanoelectronics, as they possess the potential for creating high-density devices with low power consumption in combination with high operative speed. Moreover, because of their complex internal molecular structure and the possibility of coupling different chemical functions, molecules may provide novel intrinsic functionality not found in conventional silicon electronics. The use of photofunctional molecules is particularly envisaged in view of applications for optoelectronic devices. One target among others is the conception of organic photoconductors and photoswitched conductors. An interesting approach is to incorporate a photochromic molecular system within a conducting polymer chain. Conducting polymers are very attractive materials among the different candidates for molecular wires. Their electrical conductivity can be controlled over the full range from insulator to metal by chemical or electrochemical doping.^{4,5} They can be synthesized

CHART 1



with highly controlled lengths and can be integrated in complex circuits by chemically bonding with other functional molecules without changing their electronic properties. On the other hand, photochromic molecules can behave as photoactivated electronic switches. In fact, electronic conjugation between two polymer half-chains attached to a photochromic molecule at strategic positions can be, in principle, activated or deactivated by light irradiation via the photochromic transformation.

This concept is at the origin of the recent synthesis of a series of model compounds elaborated by appending oligothiophenic chains to various photochromic 3H-naphtho[2,1-*b*]pyran molecules derived from the [2H]-chromene family (Chart 1).^{6–17} Thiophene oligomers were chosen as models of molecular wire

* Authors to whom correspondence should be addressed. E-mail: Baptiste.moine@univ-st-etienne.fr (B.M.); olivier.poizat@univ-lille1.fr (O.P.).

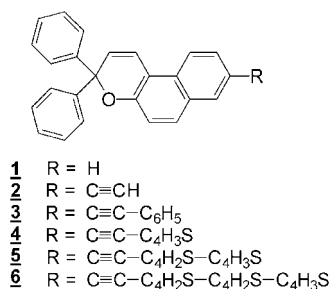
[†] Université des Sciences et Technologies de Lille.

[‡] Faculté des sciences de Luminy.

[§] Université Paul Sabatier.

^{||} Present address: Laboratoire Hubert Curien (UMR 5516 du CNRS), Université Jean Monnet de Saint-Étienne, Bât. F, 14 rue du Professeur Lauras, 42000 Saint-Étienne, France.

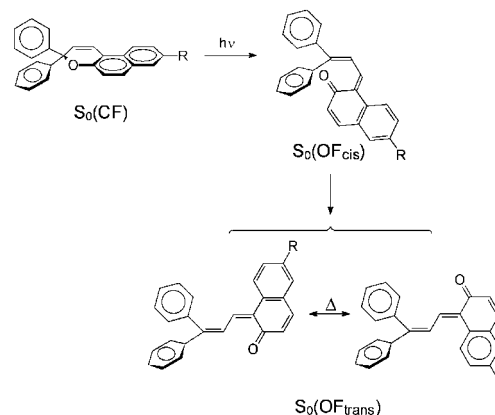
CHART 2



because, above two or three thiophene units, their conducting and semiconducting properties are similar to those of very long polythiophene chains.^{18–20} Naphthopyrans were chosen in regard to their excellent photochromic properties: high colorability, rapid thermal relaxation, and high resistance to fatigue.^{21–23} In this family, photochromism proceeds via the cleavage of the geminal diaryl carbon–oxygen single bond (C₃–O) of the chromene moiety.^{23,24} The reaction leads to a mixture of colored merocyanine isomers (open forms, OF) with extended π conjugation that might couple electronically substituents in positions 3 and 8 that are uncoupled in the closed form (CF). A molecular photoswitch behavior has been actually demonstrated for a 3H-naphtho[2,1-*b*]pyran compound substituted by bithiophenic groups in positions 3 and 8, with the observation of a very strong current density variation upon irradiation.^{12,13} However it has also been observed that the efficiency of photocolability of the molecule decreases markedly or even vanishes when the substituted oligothiophenic chains become too long. This failing has been particularly evidenced in a series of 3,3-diphenyl-3H-naphtho[2,1-*b*]pyrans substituted in position 8 by thiophene oligomers via an acetylenic junction: the photocolability increases progressively as the number *n* of oligomeric thiophenic substituents increases from 0 to 2, but for *n* = 3 the compound does not show any photochromism.^{8–10,15} In parallel, it was observed that the fluorescence intensity of the closed form increases continuously from *n* = 1 to 3.¹⁰ Thus, the presence of electron-conducting groups substituted on the photochromic nucleus appears to annihilate the photochromic behavior, which prevents at the moment any attempt to further develop such devices. To be able to remedy this lost of functionality, it is essential to understand the underlying photophysics and correlate chemical structure and functionality.

For this purpose, we present in this paper a comparative analysis by transient UV–visible absorption spectroscopy in the femtosecond to microsecond time domain of the photo-physical and photochemical properties of three 3,3-diphenyl-3H-naphtho[2,1-*b*]pyran compounds substituted in position 8 by thiophene oligomers (*n* = 1–3 units) via an acetylenic junction (compounds **4**, **5**, and **6**, respectively, in Chart 2) in solution. For comparison, the simple ethynyl-substituted molecule **2** (*n* = 0 analogue) has also been investigated. The overall aim of this analysis is to determine the photochromism mechanism and elucidate, at the molecular level, the factors that control the photochromism efficiency. A schematic representation of the photochromic reaction process expected in this family of compounds is shown in Scheme 1. The existence of two trans isomers of the photomerocyanine product (open forms, OF_{trans}) in thermal equilibrium has been confirmed from NMR studies in the case of compounds **2**, **4**, and **5**.²⁵

The results obtained in this work for compounds **2**, **4**, **5**, and **6** are discussed by analogy with those recently reported for the unsubstituted parent molecule (**1** in Chart 2)^{26,27} and for the

SCHEME 1: Geometrical Representation of the Ground-State CF and *cis/trans* OFs of the 3,3-Diphenyl-3H-naphtho[2,1-*b*]pyran Compounds

compound substituted in position 8 by a phenylethynyl group (**3** in Chart 2).²⁸ Partial results obtained for the dithienylethynyl substituted compound **5** have been the object of a previous short communication.²⁹

Experimental Methods

Synthesis and purification of 3,3-diphenyl-3H-naphtho[2,1-*b*]pyran substituted in position 8 by ethynyl (**2**), thienylethynyl (**4**), dithienylethynyl (**5**), and terthienylethynyl (**6**) groups was reported previously.^{8,9} Acetonitrile (CH₃CN) and cyclohexane (C₆H₁₂) (Aldrich, spectrophotometric grade) were used without further purification.

The femtosecond transient absorption setup has been already described.³⁰ Briefly, it involves a 1-kHz Ti–sapphire laser system based upon a Coherent (MIRA 900D) oscillator and a BM Industries (ALPHA 1000) regenerative amplifier. Pump excitation at 377 and 266 nm (~150 fs, 3–15 μ J per pulse, 0.3–1.5 mJ/cm²) was obtained by frequency doubling the Ti–sapphire fundamental tuned at 754 nm or frequency tripling the fundamental tuned at 800 nm, respectively (0.3 mm BBO crystals). A white light continuum probe pulse was generated by focusing the 754- or 800-nm beam in a 1-mm CaF₂ plate. The pump–probe polarization configuration was set at the magic angle (54.7°). The probe–pulse was delayed in time relative to the pump pulse using an optical delay line (Microcontrol Model MT160–250PP driven by an ITL09 controller, precision \pm 1 μ m). The overall time resolution (fwhm of the pump–probe intensity cross-correlation) was estimated to be about 300 fs from the two-photon (pump + probe) absorption signal in pure hexane. The time dispersion of the continuum light over the 300–700-nm region of analysis was about 0.8 ps. The transmitted light was analyzed by a charge-coupled device (CCD) optical multichannel analyzer (Princeton Instrument LN/CCD-1340/400-EB detector + ST-138 controller). Sample solutions (2.5 \times 10^{–4} M) were circulating in a flow cell equipped with 0.2 mm thick CaF₂ windows and characterized by a 2-mm optical path length. Data were accumulated over 3 min (~180000 pump–probe sequences).

Nano-microsecond transient absorption experiments were performed using a laser flash photolysis apparatus. Excitation pulses at 355 and 266 nm (7–8 ns, 1 mJ) were provided by a 20-Hz Nd:YAG laser (DIVA II, Thales laser). The probe light was provided by a Xe flash lamp (XBO 150W/CR OFR, OSRAM). Samples were contained in a quartz cell (10 \times 10 mm² section) at a concentration adjusted to get an OD value of

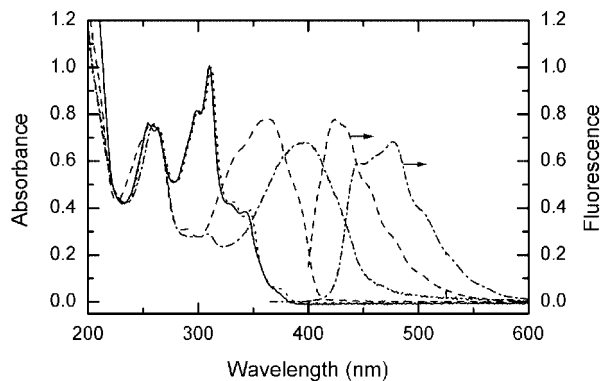


Figure 1. Normalized absorption spectra (left axis) of **2** (solid line), **4** (dotted line), **5** (dashed line), and **6** (dash-dot line) in acetonitrile. Normalized fluorescence spectra (right axis) of **5** (dashed line) and **6** (dash-dot line) are also shown.

~ 1.0 at the pump excitation wavelength. All solutions were deaerated by bubbling N_2 apart from those used for measuring the effect of quenching by O_2 . The transmitted light was analyzed with a photomultiplier (R1477-06, Hamamatsu) coupled to a digitalized oscilloscope (TDS 540, Tektronix). The triplet state quantum yield (ϕ_T) and extinction coefficient (ϵ_T) were obtained by comparing the changes in absorbance related to the formation of triplet β -carotene via sensitization by triplet energy transfer from benzophenone (reference solution) on one hand and from the photochromic compound on the other hand, after excitation at 355 nm. Both measurements were done at the same conditions of irradiation, absorbance at 355 nm, and concentration of β -carotene.³¹⁻³³ Benzophenone was used as a standard of unitary triplet yield and a ϵ_T value of $6500 \text{ M}^{-1} \text{ cm}^{-1}$ at 525 nm.³⁴

The quantum yield of the photoreaction leading to the open form, OF_{trans} (or photocoloration quantum yield, Φ_R), and the molar absorption coefficient (ϵ_{OF}) of OF_{trans} (assuming same ϵ_{OF} value for both isomers) were determined from steady state photolysis measurements performed on low-concentrated solutions ($\sim 10^{-4} \text{ M}$) using an already described experimental setup.^{35,36} Irradiation of the samples using a Xe lamp was achieved in a 10-mm path thermostatted cell at right angle to the monitoring beam (HP mercury lamp). The irradiation wavelength was tuned at the absorption maximum of the open form of the photochromic compounds by using interferential filters. Absorption changes were measured with an Ocean Optics spectrophotometer.

Results

Figure 1 shows the absorption spectra of **2**, **4**, **5**, and **6** in acetonitrile, and the fluorescence spectra of **5** and **6**. No significant fluorescence emission could be detected for **2** and **4**. The absorption spectra are characterized by three groups of bands in the 200–400-nm region: an intense absorption peaking below 200 nm, a narrow band centered around 260 nm, almost constant in the four compounds, and a broader band with more or less complex vibronic structure lying above 300 nm. This latter band has strictly similar shape and position in compounds **2** and **4** ($\lambda_{\text{max}} = 310 \text{ nm}$). It is roughly lying in the same region as the lowest energy band in the parent, unsubstituted compound **1**²⁷ and can thus be considered as characteristic of the 3H-naphtho[2,1-*b*]pyran photochromic nucleus. However, this band appears notably red-shifted on going to **5** ($\lambda_{\text{max}} 362 \text{ nm}$) and then to **6** ($\lambda_{\text{max}} 398 \text{ nm}$). Its assignment to the $S_0 \rightarrow S_1$ transition is clearly established by the manifest mirror image aspect of

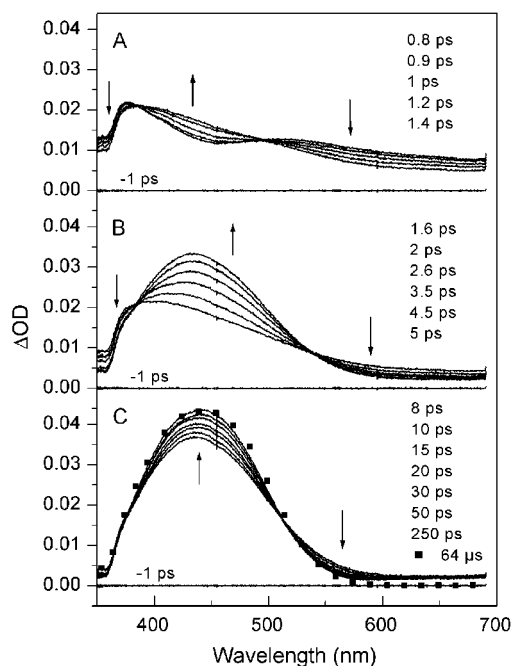


Figure 2. Transient absorption spectra of **2** in acetonitrile at different time delays from 0.8 to 1.4 ps (A), 1.6–5 ps (B), and 8–250 ps (C) after excitation at 266 nm. Vertical arrows indicate the signal evolution. The spectrum obtained at 64 μs from laser flash photolysis experiment is also shown for comparison in part C.

the fluorescence spectrum of **5** ($\lambda_{\text{max}} 424 \text{ nm}$) and **6** ($\lambda_{\text{max}} 476 \text{ nm}$, high energy shoulder at $\sim 445 \text{ nm}$). The progressive red-shift characterizing the absorption and fluorescence band maxima on going from **4** to **5** and then to **6** reveals an increasing stabilization of the S_1 state relative to S_0 upon enlarging the oligothiophenic chain from 1 to 3 units, i.e., an increasing degree of electronic conjugation between the thiophenic chain and the 3H-naphtho[2,1-*b*]pyran photochromic group. The involvement of the thiophenic oligomer in the chromophore is corroborated by the observation that both the emission band shape and the almost symmetrical and structureless $S_0 \rightarrow S_1$ absorption band shape in **5** and **6** show some resemblance with the absorption³⁷ and emission^{38,39} band shapes of the bithiophene (**2T**) and terthiophene (**3T**) molecules, respectively, in solution. The notable red shift of these absorption and emission features in **5** and **6** relative to **2T** ($\lambda_{\text{max}}(\text{abs}) 300 \text{ nm}$, $\lambda_{\text{max}}(\text{flu}) 360 \text{ nm}$) and **3T** ($\lambda_{\text{max}}(\text{abs}) 350 \text{ nm}$, $\lambda_{\text{max}}(\text{flu}) 430 \text{ nm}$) reflects the conjugation with the 3H-naphtho[2,1-*b*]pyran part.

3,3-Diphenyl-8-(ethynyl)-3H-naphtho[2,1-*b*]pyran (2) and 3,3-Diphenyl-8-(thienylethynyl)-3H-naphtho[2,1-*b*]pyran (4). Femto-picosecond transient absorption spectra recorded in the 350–700-nm domain for the ethynyl substituted compound **2** in acetonitrile at different time delays from 0.8 to 250 ps following 266-nm excitation are shown in Figure 2. Three steps can be noticed in the spectral evolution. The initial spectrum at 0.8 ps presents two broad bands at 375 and 515 nm. It decays with a time constant t_1 of $0.5 \pm 0.1 \text{ ps}$, as measured in the 540–700-nm region, to yield a new broad spectrum (1.4-ps trace) showing a single maximum at 390 nm and a long red tail up to 700 nm. Two approximate isosbestic points characterize this evolution at 386 and 495 nm (Figure 2A). Then, in the 1.8–100-ps time range, this spectrum transforms gradually into a third one showing a well-defined band centered at 440 nm that rises essentially with a bi-exponential kinetics of time constants $t_2 = 2.3 \pm 0.2 \text{ ps}$ and $t_3 = 17 \pm 4 \text{ ps}$, respectively. Two isosbestic points at 385 and 540 nm characterize the faster

TABLE 1: Time Constants (ps) and Position of the Open form Absorption Maximum (nm) for the 3,3-Diphenyl-3H-naphtho[2,1-*b*]pyran Compounds Defined in Chart 2 (Acetonitrile Solvent)

	t_1 (ps)	t_2 (ps)	t_3 (ps)	$\lambda_{\max}(\text{OF})$ (nm)
1	0.45	1.8	21	425
2	0.5	2.3	17	440
3	0.28	2.0	10	460
4	0.4	2.5	16	460
5	105			485
6	300			

kinetics (Figure 2B) while only one is observed at 512 nm for the slower kinetics (Figure 2C). After 100 ps, no significant spectral change occurs up to 1500 ps. Moreover, as can be seen in Figure 2C, the 64- μs spectrum recorded by using the laser flash photolysis experiment is comparable to the 100-ps spectrum and does not show any evolution over the 0.5–100- μs time domain, in aerated solution as well as in N_2 -purged solution. Similar spectrokinetic evolution is found for the thienylethynyl substituted compound **4**, with characteristic times close to those found for **2** (see Table 1).

Quite similar spectrokinetic properties were also observed previously for the phenylethynyl compound **3**²⁸ and the unsubstituted parent compound **1**.^{26,27} The analogy concerns the spectral characteristics as well as the overall dynamics. In particular, in all cases, the same three steps are observed in the spectral evolution with comparable time constants (t_1 – t_3), as can be seen in Table 1. The position of the final absorption band remaining after 100 ps is also given in table 1 (440 nm in **2**, 460 nm in **4**). It corresponds without doubt to the spectrum of the thermally equilibrated trans merocyanine isomer mixture (open forms $S_0(\text{OF}_{\text{trans}})$, see Scheme 1) that has been identified elsewhere from continuous irradiation measurements.⁸ The species that precedes the formation of $S_0(\text{OF})$ (third step of the spectral evolution, Figure 2C) has a very similar spectrum (8 ps trace) and must have close structure. As proposed for **1**^{26,27} and **3**,²⁸ the third reaction step (time t_3) is thus likely characterizing some kind of conformational evolution of the open forms toward the final thermal equilibrium. On the other hand, again by analogy with the previous results reported for **1** and **3**, the initial and very short-lived spectrum observed after photoexcitation (0.8 ps trace in Figure 2A) can be ascribed to the lowest excited singlet state of CF, $S_1(\text{CF})$. The time constant t_1 corresponds thus to the S_1 state lifetime of the closed form. It is clear that, as previously observed for **1**²⁶ and **3**,²⁸ the decay time t_1 does not match any one of the two growing times t_2 and t_3 of the final $S_0(\text{OF})$ spectrum, which implies the existence of an intermediate species characterized, in Figure 2A, by the broad and diffuse spectrum observed at 1.4 ps. The identity of this species will be discussed below (see Discussion section). Note that, in all compounds **1**–**4**, OF is the only apparent photo-product, suggesting a nearly unity quantum yield for the excited-state ring-opening reaction. This result is in agreement with the very short lifetime of $S_1(\text{CF})$ in these compounds: the ultrafast ring-opening reaction quenches all other possible deactivation pathway of S_1 such as emission or intersystem crossing (ISC).

3,3-Diphenyl-8-(terthienylethynyl)-3H-naphtho[2,1-*b*]pyran (6**)**. Femto-picosecond transient absorption spectra recorded in the 385–730-nm domain for the terthienylethynyl substituted compound **6** in acetonitrile at different time delays from 5 to 1500 ps following 377 nm excitation are shown in Figure 3. No significant spectral evolution is observed at times shorter than 5 ps. The 5 ps spectrum shows a strong negative band ($\lambda_{\max} = 476$ nm, shoulders at ~ 448 and ~ 505 nm) readily

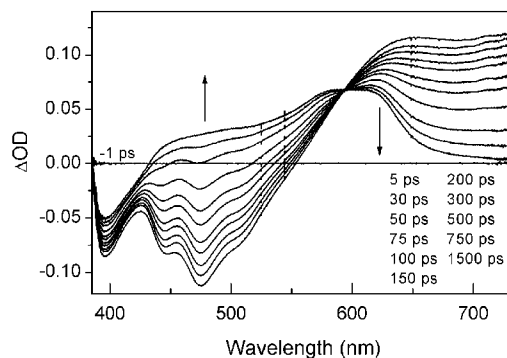


Figure 3. Transient absorption spectra of **6** in acetonitrile at different time delays from 5 to 1500 ps after excitation at 377 nm. Vertical arrows indicate the signal evolution.

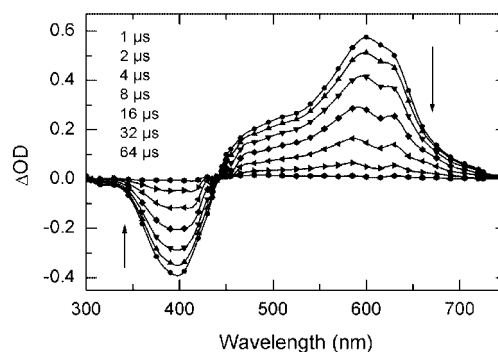


Figure 4. Laser flash photolysis spectra obtained from 1 to 64 μs after 355-nm excitation of a deaerated solution of **6** in acetonitrile. Vertical arrows indicate the signal evolution.

ascribed to stimulated emission ($S_1 \rightarrow S_0$) as it matches rigorously the fluorescence spectrum of **6** (see Figure 1), a weaker negative band (λ_{\max} 395 nm) assigned with certainty to the ground-state bleach as it corresponds to the ground-state absorption of **6** (dash-dot trace in Figure 1), and a broad positive signal showing a smooth maximum at 650 nm and a second band extending beyond 730 nm. In conformity with the presence of a perfect isosbestic point at 594 nm, the transient absorption and stimulated emission bands are found to decay with the same single-exponential kinetics of time constant 300 ± 10 ps. The absorption signal, as the emission, is thus characterizing the $S_1(\text{CF})$ state and can be assigned to $S_1 \rightarrow S_n$ transitions. Note that, although three conformations syn–syn, syn–anti, and anti–anti are in principle expected for the terthienyl moiety,⁴⁰ the corresponding three conformers of **6** cannot be differentiated by specific S_1 state decay kinetics. It is worth noticing that the 300-ps S_1 lifetime measured for **6** (time t_1 in Table 1) is almost 3 orders of magnitude longer than the S_1 lifetimes found above for **2** and **4**.

The spectrum obtained after a complete decay of S_1 (1500 ps spectrum in Figure 3) shows a new transient absorption band maximizing around 600 nm together with a residual bleaching component at 395 nm. This spectrum corresponds precisely to that obtained at 0.5 μs by flash photolysis (Figure 4). At longer times, the 600-nm absorption and bleaching bands decay simultaneously with a common single-exponential kinetics of 16.8 μs in deoxygenated solution. Much shorter decay is found in the presence of O_2 , which suggests that the 600 nm band is due to a triplet state absorption ($T_1 \rightarrow T_n$) of CF. This hypothesis was confirmed by sensitization experiments with benzophenone. After total decay of the T_1 spectrum, the bleach component has also entirely disappeared, and no residual transient signal is observed (80 μs spectrum in Figure 4). This result indi-

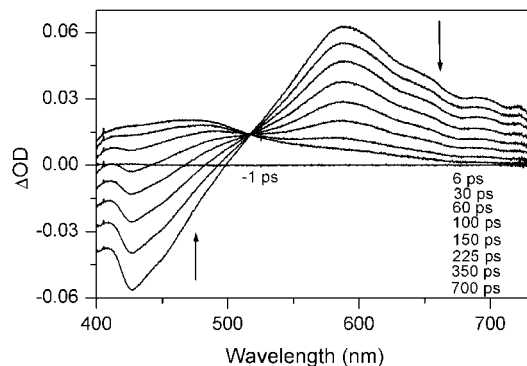


Figure 5. Transient absorption spectra of **5** in acetonitrile at different time delays from 6 to 700 ps after excitation at 377 nm. Vertical arrows indicate the signal evolution.

ates that complete repopulation of the initial CF ground state is achieved. The behavior of **6** upon photoexcitation is thus restricted to common photophysical relaxation of $S_1(\text{CF})$ via competing radiative and nonradiative (ISC to T_1) processes. The lack of any spectral evidence of the formation, even transiently, of an OF product after photoexcitation is consistent with the absence of photochromic properties reported for **6**^{8,10} and reveals that this inactivity results from the fact that the ring opening reaction does not occur rather than from a low stability of the OF species.

3,3-Diphenyl-8-(dithienylethynyl)-3H-naphtho[2,1-*b*]pyran (5). Femto-picosecond transient absorption spectra recorded in the 400–730-nm region for the dithienylethynyl substituted compound **5** in acetonitrile at different time delays from 6 to 700 ps following 377 nm excitation are shown in Figure 5. The general aspect of the short-time spectrum (6 ps) resembles that observed for **6** with a negative band in the blue region and a positive one in the red region. The former presents a peak at 425 nm and an unresolved shoulder at ~450 nm and can be ascribed to the stimulated emission by analogy with the fluorescence spectrum of **6** (Figure 1). Moreover, a negative UV band, the edge of which is discerned around 400 nm, is likely due to the ground-state bleach. The strong absorption band peaking at 585 nm is assigned to the CF S_1 state absorption as it decays concomitantly with the stimulated emission (time constant $t_1 = 105 \pm 2$ ps, isosbestic point at 515 nm). As in the case of **6**, the two conformers of **5** characterized by conformations syn and anti of the dithienyl moiety are not differentiated by specific S_1 state decay kinetics.

After full decay of S_1 (700 ps spectrum in Figure 3), one observes a new spectrum showing a band at 470 nm and a weak, unresolved shoulder at ~610 nm. This spectrum corresponds clearly to that obtained at 0.5 μs from flash photolysis measurements (Figure 6A). The larger spectral window available by flash photolysis in the UV region reveals the presence, in addition to the above absorption features, of a negative band at 365 nm and a shoulder around 335 nm that is unambiguously due to the ground-state bleach. The time evolution observed in the microsecond domain shows the partial decay of the bleach and of the absorption with a common kinetics of 14.0 ± 0.2 μs in deaerated acetonitrile solution. This kinetics being notably faster in the presence of O_2 , it can be assumed, as in the case of **6**, to characterize the decay of the triplet (T_1) state of CF. However, in contrast to what was observed for **6**, a strong residual spectrum is still present after complete decay of the T_1 state (64 μs spectrum in Figure 6A). If the 610-nm absorption component has totally disappeared, this spectrum shows some bleach contribution and the most of the initial 470 nm absorption

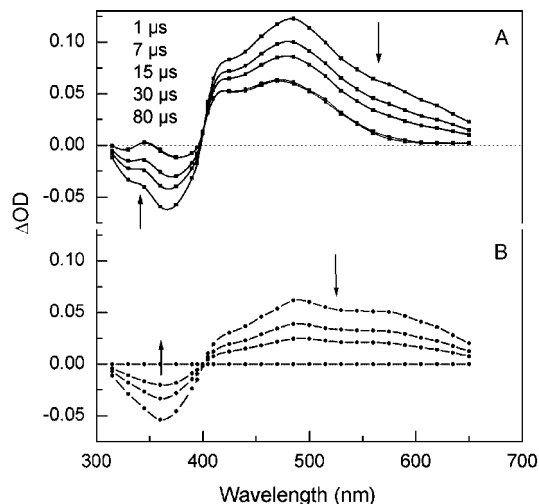


Figure 6. Laser flash photolysis spectra obtained from 1 to 80 μs after 355-nm excitation of a deaerated solution of **5** in acetonitrile: (A) raw spectra; (B) spectra processed by subtracting the 64 μs spectrum at all times. Vertical arrows indicate the signal evolution.

TABLE 2: Triplet Quantum Yield Φ_T , Photocoloration Quantum Yield Φ_R , Molar Absorption Coefficients ϵ_{CF} ⁹ and ϵ_{OF} at λ_{max} , Relative Fluorescence Intensity $I_{\text{F}}^{\text{rel}}$,¹⁰ and Colorability A_0 ⁹ for Compounds 4–6 in Acetonitrile

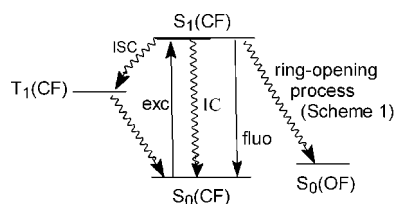
	$\epsilon_{\text{CF}} (\lambda_{\text{max}})$	$\epsilon_{\text{OF}} (\lambda_{\text{max}})$	ϕ_R	ϕ_T	$I_{\text{F}}^{\text{rel}}$	A_0
4	17000 (310 nm)	21500 (460 nm)	0.76	0	0	3.1
5	28000 (362 nm)	22500 (485 nm)	0.7	0.1	0.29	5.3
6	30000 (398 nm)		0	0.6	0.6	0

band. Its amplitude is constant on the millisecond time scale. This stability is unaffected by the presence of oxygen in the solution. The 470-nm absorption is characteristic of the merocyanine species, $S_0(\text{OF})$, previously identified from continuous irradiation measurements.⁸ By analogy with the photoinduced reaction mechanism established for compounds 1–4 (see Discussion section), in which the ring-opening process arises from the excited singlet state $S_1(\text{CF})$, the OF product in **5** can also be assumed to be formed entirely from the S_1 state, with a time constant of 105 ps, and to keep a constant concentration at longer time. Therefore, a constant spectral contribution of $S_0(\text{OF})$, corresponding to the 64 μs spectrum in Figure 6A, is expected to be present at all times in the microsecond time domain. Subtracting the 64 μs spectrum to all spectra in Figure 6A leads to the spectral evolution displayed in 6B that is thus purely characterizing the T_1 state contribution. As a matter of fact, the same T_1 state spectrum was observed from triplet–triplet energy transfer experiments using benzophenone as triplet sensitizer, confirming definitely the above assignment.

In summary, the photoexcited $S_1(\text{CF})$ state of **5** relaxes via three competing deactivation pathways: direct repopulation of the CF ground-state by radiative emission, ISC to the CF triplet state followed by triplet deactivation toward the CF ground state, and formation of the OF ground-state product by the ring-opening reaction.

The triplet quantum yield Φ_T , photocoloration quantum yield Φ_R , and open form molar absorption coefficient ϵ_{OF} measured for compounds 4–6^{9,10} are given in Table 2. Values previously reported for the molar absorption coefficient ϵ_{CF} and relative fluorescence intensity $I_{\text{F}}^{\text{rel}}$ of the closed form and for the colorability A_0 are also presented in Table 2. Contrary to ϕ_T and Φ_R , $I_{\text{F}}^{\text{rel}}$ is not a quantum yield but a qualitative estimate of the fluorescence intensity measured relative to the intensity

SCHEME 2: Schematic Representation of the Radiative (Straight Lines) and Nonradiative (Zigzag Lines) Relaxation Processes after UV Excitation of the 3,3-Diphenyl-3H-naphtho[2,1-*b*]pyran Compounds



of the most emissive compound in the family of the 8-substituted 3,3-diphenyl-3H-naphtho[2,1-*b*]pyrans.¹⁰ The A_0 parameter corresponds to the experimental absorption intensity of the colored merocyanine photoproduct ($S_1(\text{OF})$) measured at the $\lambda_{\text{max}}(\text{OF})$ (see Table 1) after calibrated flash excitation of the compound.⁴¹ It provides a quantitative estimate of the intrinsic photochromism efficiency of a compound and can be expressed by

$$A_0 = K \varepsilon_{\text{CF}} \varepsilon_{\text{OF}} \Phi_{\text{R}}[\text{CF}] \quad (1)$$

where K is a constant and $[\text{CF}]$ is the initial concentration of the photochromic compound in the closed form.

A last question concerns a possible contribution of two-photon absorption processes in the photoinduced reactivity. In fact, the nonlinear response of organic molecules usually rises with the π -electron density delocalization. An increasing contribution of nonlinear optical effects with the extension of the π -conjugated chain on going from **1** to **6** could thus be possible. However, these effects can be considered as negligible in our experimental conditions as the transient absorption signals measured for all samples have intensity varying linearly with the pump intensity in the 3–15- μJ range experienced.

Discussion

From the above results, the photoinduced reactivity of the investigated 3,3-diphenyl-3H-naphtho[2,1-*b*]pyran compounds can be recapitulated by the common reaction scheme 2. However the compounds appear to differ drastically from each others by the relative magnitude of the photochemical (ring-opening process) vs photophysical (fluorescence, ISC) excited-state relaxation pathways. Compound **5** is intermediate between **2** and **4** (and also **1** and **3**) on one hand, that lead exclusively to the merocyanine OF product (quantum yield for the photochemical route close to unity), and **6**, on the other hand, that is not photochromic (quantum yield for the photochemical route close to zero), and relaxes entirely via fluorescence and ISC. There is an inverse relationship between the excited-state lifetime (t_1 in Table 1) and the reaction efficiency, which indicates a kinetic control of the reactivity. In compounds **1–4**, ultrafast ring-opening reaction leads to sub-picosecond deactivation of the $S_1(\text{CF})$ state and quenches entirely the emission and ISC processes. Inversely, in **6**, the reaction is much slower than emission and ISC and does not occur with significant yield during the $S_1(\text{CF})$ state lifetime. These observations denote the existence of an excited-state potential barrier along the ring-opening reaction coordinate that vary considerably with the length n of the oligothiophenic chain substituted to the naphtho[2,1-*b*]pyran group. Whereas the reaction is almost barrierless for $n \leq 1$ (compounds **1–4**, S_1 lifetime < 1 ps), the barrier increases notably for $n = 2$ (compound **5**, S_1 lifetime = 105 ps) and $n = 3$ (compound **6**, S_1 lifetime = 300 ps). Before analyzing in more detail the influence of the oligothiophenic

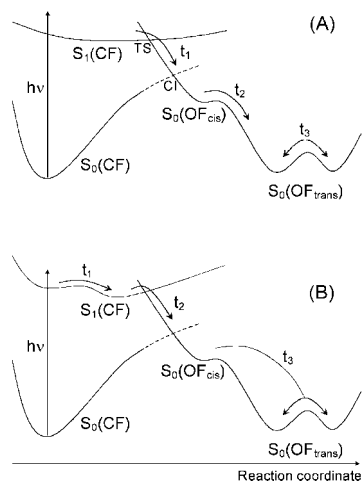
chain length on the ring-opening reaction efficiency, the mechanism of this reaction must be discussed.

Mechanism of the Ring-Opening Process. The transient absorption data obtained for compounds **2** and **4** have revealed the existence of three well-defined steps in the photoinduced process responsible for the photochromic behavior, characterized by time constants t_1 to t_3 , respectively. If step 3 has been ascribed without ambiguity to a ground-state conformational evolution of the OF species toward the final trans isomer mixture at thermal equilibrium, steps 1 and 2 remain indeterminate. Their nature depends on the identity of the short-lived transient species produced in step 1 from the decay of $S_1(\text{CF})$. The clear analogy observed in the spectral evolution of compounds **2** and **4** on one hand and **1**^{26,27} and **3**²⁸ on the other hand, following pulse laser excitation, indicates unambiguously that the same reaction mechanism takes place in all cases. We thus propose to transfer to compounds **2** and **4** the reaction scheme recently proposed for **1** and **3**²⁸ from the combined analysis of experimental data and CASSCF calculations of the excited-state ring-opening reaction coordinate in the model molecule [2H]-chromene (Chart 1).^{27,42} According to this previous report, two plausible assignments can be suggested for the short-lived species immediately following the initially produced $S_1(\text{CF})$ state. First, it can be a metastable ground-state cisoid OF isomer, $S_0(\text{OF}_{\text{cis}})$, corresponding to the first expected product of the ring-opening reaction (see Scheme 1). This assignment is consistent with the CASSCF prediction for [2H]-chromene²⁷ that the excited $S_1(\pi\pi^*)$ state surface presents a rather flat region with very shallow and indefinite minimum extending from the initial Franck–Condon excitation region to a transition state (TS) that leads directly and without significant barrier to a conical intersection (CI) with the ground-state surface. The TS point marks a transition of the excited-state from $\pi\pi^*$ to $n\pi^*$ nature (S_1/S_2 avoided crossing), the $n\pi^*$ surface being dissociative along the $\text{C}_3\text{—O}$ bond. In this hypothesis, the initial $S_1(\text{CF})$ species identified experimentally corresponds to the shallow excited $\pi\pi^*$ state minimum and its ultrafast decay (time t_1) is due to the near barrierless ring-opening process. Then, the t_2 and t_3 time constants can be associated to the kinetics of ground-state cis–trans isomerization of the OF species and of thermal equilibrium between two possible trans forms, OF_{trans} , respectively. This reaction pathway is schematically represented in Scheme 3A.

An alternative interpretation rests on the hypothesis that the excited-state surface might be more complex than that predicted for [2H]-chromene with, for instance, a weak barrier between an excited state minimum close to the Franck–Condon region and a second shallow minimum farther on the excited surface, before the transition state toward the $n\pi^*$ surface. This reaction pathway is depicted in Scheme 3B. In this case the t_1 time constant could correspond to a restricted excited-state structural relaxation toward this second minimum, the t_2 component to the ring-opening process (crossing of the transition state), and the t_3 contribution to the overall ground-state evolution (cis–trans isomerization and thermal equilibrium between the trans forms). In this interpretation, the first two transient species belong to the excited-state potential surface, which appears consistent with the resemblance of their broad spectra (0.8 and 1.4 ps traces, respectively, in Figure 2) that contrasts with the well-defined spectra of the subsequent ground-state open forms.

In **5**, the mechanism of the ring-opening reaction is logically expected to be the same as in **1–4**. The fact that no kinetic component corresponding to steps 2 and 3 was observed in the spectral evolution of **5** can be interpreted as an effect of the

SCHEME 3: Schematic Representation of the Two Reaction Pathways Envisaged for the Ring-Opening Process Based on the Absence (A) or Presence (B) of an Excited-State Reaction Step Precursor to the Ring-Opening Process



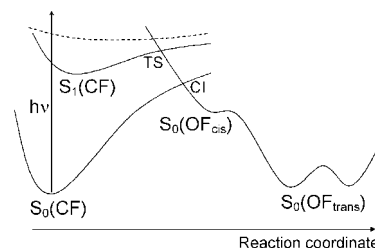
much longer S_1 state lifetime in this compound ($t_1 = 105$ ps). Assuming that steps 2 and 3 are as fast in **5** as in compounds **1–4**, their kinetics become unresolved in the case of **5** because they are much shorter than the kinetics of the earlier step 1.

Influence of the Oligothiophenic Chain on the Reaction Pathway. One observes (see Table 1) a progressive red shift of the visible absorption band of the OF photoproduct upon increasing the length n of the substituted oligothiophenic chain, from 425 nm for the unsubstituted compound **1** to 485 nm for the $n = 2$ compound **5**. This bathochromic effect is indicative of the existence of π conjugation between the substituted chain and the π system of the opened form of the naphthopyran moiety. Such an extended π -electron delocalization is potentially favorable to the existence of some electronic conductivity in the OF form, which was one of the properties expected when elaborating this type of molecular systems.

On the other hand, the notable red-shifts of the CF absorption and fluorescence band maxima on going from **4** to **5** and then to **6** (Figure 1) reflects a progressive stabilization in energy of the $S_1(\pi\pi^*)$ state relative to S_0 that reveals an increasing degree of electronic π conjugation between the oligothiophenic chain and the 3H-naphtho[2,1-*b*]pyran moiety also in the CF form. Whichever the hypothesis of one or two shallow minima on the $S_1(\pi\pi^*)$ surface (part A or B of Scheme 3), a stabilization of this surface might result in the emergence of a barrier at the transition state TS formed at the $\pi\pi^*/n\pi\pi^*$ crossing. Accordingly, starting from the near barrierless reaction parts A or B of Schemes 3 envisaged for compounds **1–4**, an extension of the oligothiophenic chain length from 1 to 3 thiophene units is expected to increase the energy barrier between the S_1 minimum and TS, as shown in Scheme 4. This π -conjugation effect might explain the n -dependent excited-state potential barrier that has been shown to appear along the ring-opening reaction coordinate. Beside this effect of stabilization of the S_1 state geometry, a further consequence of the π -conjugation is a larger spatial extension of the π -chromophore that is less localized on the photochromic part of the molecule, in such a way that the energy deposited in the S_1 state is potentially less beneficial to the ring-opening reaction.

Comparison of the Φ_R , Φ_T , and I_F^{rel} values in Table 2 confirms that concomitant intensification of the ISC and emission processes parallels the reduction of the open-ring

SCHEME 4: Schematic Representation of the Effect of Electronic π Conjugation between the Oligothiophenic Chain and the 3H-Naphtho[2,1-*b*]pyran Moiety on the Excited State Surface^a



^a The dashed line represents the S_1 state surface in absence of π conjugation (similar as in Scheme 3A).

reaction efficiency as the oligothiophenic chain length rises. In compound **4**, the absence of any perceptible emission and triplet state formation ($\Phi_T \sim 0$, $I_F^{\text{rel}} \sim 0$) is consistent with an ultrafast deactivation of $S_1(\text{CF})$ due to the near barrierless reaction process (S_1 lifetime 0.4 ps). As mentioned above, a quantum yield for the photochemical route close to unity is thus likely, which means that 100% of the excited molecules quit the $S_1(\pi\pi^*)$ surface by crossing the TS point along the reaction coordinate (see Scheme 3). However, the fact that the quantum yield Φ_R of formation of the open form is only 0.76 reveals that, at the CI, only three-fourth of these molecules continue their way along the reaction coordinate on the $S_0(\text{OF})$ surface and undergo complete ring-opening reaction, one-fourth of the molecules going back to the initial $S_0(\text{CF})$ surface minimum. In compound **5**, despite the observation of some ISC and emission and of a much longer S_1 state lifetime (105 ps) caused by the existence of a significant barrier to the reaction, the photochemical route remains the dominant S_1 state decay pathway with a quantum yield Φ_R only slightly smaller than in **4**. In any way, the notable increase in colorability (A_0) found on going from **4** to **5** cannot be imputed to an enhancement of the open-ring reaction efficiency but, according to the definition of A_0 (1), is rather reflecting the increase of the ground-state absorbance (ϵ_{CF}) of the closed form that surpasses largely the diminution of Φ_R . Finally, in compound **6**, the total loss of photochromic behavior ($A_0 = 0$) can be unambiguously ascribed to the inhibition of the ring-opening reaction. The sudden drop of the reaction yield Φ_R on going from **5** to **6** suggests that the barrier to the ring-opening process has reached in **6** a threshold that cannot be overcome.

Conclusion

The spectroscopic investigation of 3,3-diphenyl-3H-naphtho[2,1-*b*]pyran compounds substituted in position 8 by thiophene oligomers ($n = 0–3$ units) via an acetylenic junction has confirmed the fact that some electronic conjugation between the naphthopyran and oligothiophenic moieties characterizes the colored (open) form, which is in principle favorable to the existence of conduction properties. However this encouraging result is thwarted by the total disappearance of the photochromic characteristics typical of the naphthopyran part for oligothiophenic chain length $n > 2$.

From the analysis of the photophysical and photochemical properties of these compounds investigated in solution by transient absorption spectroscopy, the loss of the photochromic behavior has been shown to be of electronic origin. It is assumed to be due to the presence in the excited $S_1(\pi\pi^*)$ state of a potential barrier toward the ring-opening reaction coordinate

responsible for the photochromic effect. This barrier appears very dependent on the π -electronic distribution in the excited state. Insignificant when the chain length is shorter than $n = 2$ thiophene units, in which case the π chromophore of the $S_0 \rightarrow S_1$ transition is located essentially within the naphthopyran group, it increases notably for $n \geq 2$, probably by reason of the spatial extension of the π -chromophore on the oligothiophenic chain that stabilizes the S_1 state surface minimum. Also, in reason of this spatial extension, the energy deposited in the S_1 state is less localized in the photochromic part of the molecule and thus less efficient in promoting the ring-opening process. For $n = 2$, the loss of efficiency of this process is largely compensated by an increase in absorbance of the ground-state molecule so that the overall photochromic properties are improved compared to those of the $n = 1$ compound. However, for $n = 3$, the π -conjugation effect is strong enough to totally inhibit the reaction.

Finally, the inadequacy of the investigated family of compounds to lead to effective photoswitchable molecular conductors comes from the fact that the π conjugation between the naphthopyran and oligothiophenic moieties occurs not only in the final open form but exists already partly in the initial closed form.

Acknowledgment. The authors thank the Groupements de Recherche GDR 2466 and GDRI 93 from CNRS and the Centre d'études et de Recherches Lasers et Applications (CERLA) for their help in the development of this work. CERLA is supported by the Ministère chargé de la Recherche, Région Nord/Pas de Calais, and the Fonds Européen de Développement Economique des Régions.

References and Notes

- (1) Service, R. F. *Science* **2001**, *294*, 2442.
- (2) Nitzan, A.; Ratner, M. A. *Science* **2003**, *300*, 1384.
- (3) Martin, C. R. C. R.; Baker, L. A. *Science* **2005**, *309*, 67.
- (4) Heeger, A. J. *Angew. Chem., Int. Ed.* **2001**, *40*, 2591.
- (5) MacDiarmid, A. G. *Angew. Chem., Int. Ed.* **2001**, *40*, 2581.
- (6) Moustrou, C.; Samat, A.; Guglielmetti, R.; Dubest, R.; Garnier, F. *Helv. Chim. Acta* **1995**, *78*, 1887.
- (7) Moustrou, C.; Rebière, N.; Samat, A.; Guglielmetti, R.; Yassar, A.; Dubest, R.; Aubard, J. *Helv. Chim. Acta* **1998**, *81*, 1293.
- (8) Frigoli, M.; Moustrou, C.; Samat, A.; Guglielmetti, R. *Helv. Chim. Acta* **2000**, *83*, 3043.
- (9) Frigoli, M.; Moustrou, C.; Samat, A.; Guglielmetti, R.; Dubest, R.; Aubard, J. *J. Mol. Cryst. Liq. Cryst.* **2000**, *344*, 139.
- (10) Coen, S.; Moustrou, C.; Frigoli, M.; Julliard, M.; Samat, A.; Guglielmetti, R. *J. Photochem. Photobiol. A* **2001**, *139*, 1.
- (11) Yassar, A.; Rebière-Galy, N.; Frigoli, M.; Moustrou, C.; Samat, A.; Guglielmetti, R. *Synth. Met.* **2001**, *121*, 1463.
- (12) Yassar, A.; Rebière-Galy, N.; Frigoli, M.; Moustrou, C.; Samat, A.; Guglielmetti, R.; Jaafari, A. *Synth. Met.* **2001**, *124*, 23.
- (13) Yassar, A.; Jaafari, H.; Rebière-Galy, N.; Frigoli, M.; Moustrou, C.; Samat, A.; Guglielmetti, R. *Eur. Phys. J.: Appl. Phys.* **2002**, *18*, 3.
- (14) Yassar, A.; Garnier, F.; Jaafari, H.; Rebière-Galy, N.; Frigoli, M.; Moustrou, C.; Samat, A.; Guglielmetti, R. *Appl. Phys. Lett.* **2002**, *80*, 4297.
- (15) Carpita, A.; Lessi, A.; Rossi, R. *Synthesis* **1984**, 571.
- (16) Frigoli, M.; Pimienta, V.; Moustrou, C.; Samat, A.; Guglielmetti, R.; Aubard, J.; Maurel, F.; Micheau, J.-C. *Photochem. Photobiol. Sci.* **2003**, *2*, 888.
- (17) Frigoli, M.; Moustrou, C.; Samat, A.; Guglielmetti, R. *Eur. J. Org. Chem.* **2003**, 2799.
- (18) Garnier, F.; Horowitz, G.; Peng, X.; Fichou, D. *Adv. Mater.* **1990**, *2*, 592.
- (19) Horowitz, G.; Peng, X.; Fichou, D.; Garnier, F. *J. Mol. Electron.* **1991**, *7*, 85.
- (20) Horowitz, G.; Fichou, D.; Peng, X.; Xu, Z.; Garnier, F. *Solid State Commun.* **1989**, *72*, 381.
- (21) Bertelson, R. C. In *Techniques of Chemistry*; Brown, G. H., Ed.; Wiley: New York, 1971; Vol. 3, p 45.
- (22) Guglielmetti, J. R. In *Photochromism: Molecules and Systems*; Dürr, H., Bouas-Laurent, H., Eds.; Elsevier: Amsterdam, 1990; p 314.
- (23) Van Gemert, B. In *Organic Photochromic and Thermodynamic Compounds*; Crano, J. C., Guglielmetti, J. R., Eds.; Plenum Press: New-York, 1999; Vol. 1, p 111.
- (24) Becker, R. S.; Michl, J. *J. Am. Chem. Soc.* **1966**, *88*, 5931.
- (25) Venec, D.; Delbaere, S.; Micheau, J.-C.; Frigoli, M.; Moustrou, C.; Samat, A.; Vermeersch, G. *Photochem. Photobiol. A* **2006**, *181*, 174.
- (26) Gentili, P. L.; Danilov, E.; Ortica, F.; Rodgers, M. A. J.; Favaro, G. *Photochem. Photobiol. Sci.* **2004**, *3*, 886.
- (27) Migani, A.; Gentili, P. L.; Negri, F.; Olivucci, M.; Romani, A.; Favaro, G.; Becker, R. S. *J. Phys. Chem. A* **2005**, *109*, 8684.
- (28) Moine, B.; Buntinx, G.; Poizat, O.; Rehault, J.; Frigoli, M.; Moustrou, C.; Samat, A. *J. Phys. Org. Chem.* **2007**, *20*, 936.
- (29) Moine, B.; Buntinx, G.; Poizat, O.; Frigoli, M.; Moustrou, C.; Samat, A. *Mol. Cryst. Liq. Cryst.* **2005**, *431*, 63.
- (30) Buntinx, G.; Naskrecki, R.; Poizat, O. *J. Phys. Chem.* **1996**, *100*, 19380.
- (31) Kumar, C. V.; Qin, L.; Das, P. K. *J. Chem. Soc., Faraday Trans. 2* **1984**, *80*, 783.
- (32) Kumar, C. V.; Chattopadhyay, S. K. *J. Am. Chem. Soc.* **1983**, *105*, 5143.
- (33) Carmichael, I.; Hug, G. L. *J. Phys. Chem. Ref. Data* **1986**, *15*, 1.
- (34) Murov, S. L.; Carmichael, I.; Hug, G. L., Eds. *Handbook of Photochemistry*; Marcel Dekker: New York, 1993.
- (35) Borderie, B.; Lavabre, D.; Levy, G.; Laplante, J. P.; Micheau, J.-C. *J. Photochem. Photobiol. A* **1991**, *56*, 13.
- (36) Deniel, M. H.; Lavabre, D.; Micheau, J.-C. In *Organic Photochromic and Thermodynamic Compounds*; Crano, J. C., Guglielmetti, J. R., Eds.; Plenum Press: New York, 1999; Vol. 2, p 167.
- (37) Sease, J. W.; Zechmeister, L. *J. Am. Chem. Soc.* **1947**, *69*, 270.
- (38) Paa, W.; Yang, J.-P.; Rentsch, S. *Appl. Phys. B: Laser Opt.* **2000**, *71*, 443.
- (39) Grebner, D.; Helbig, M.; Rentsch, S. *J. Phys. Chem.* **1995**, *99*, 16991.
- (40) Aleman, C.; Julia, L. *J. Phys. Chem.* **1996**, *100* (35), 14661.
- (41) Appriou, P.; Guglielmetti, R.; Garnier, F. *J. Photochem.* **1978**, *8*, 145.
- (42) Celani, P.; Bernardi, F.; Olivucci, M.; Robb, M. A. *J. Am. Chem. Soc.* **1997**, *119*, 10815.